HEFAT2007
5th International Conference on Heat Transfer, Fluid Mechanics and Thermodynamics
Sun City, South Africa
Paper number: CS1

TRANSIENT SIMULATION OF GASEOUS PARTICLE/DROPLET LADEN FLOWS IN INDUSTRIAL-SCALE DEVICES FOR FLUE GAS CLEANING INCLUDING TWO-WAY MASS AND ENTHALPY COUPLING

Schreithofer Ch.*, Aguayo P. and Weiß Ch.
*Author for correspondence
Institute for Process Technology & Industrial Environmental Protection,
University of Leoben,
Leoben, 8700,
Austria,
E-mail: christian.schreithofer@unileoben.ac.at

ABSTRACT

The method of computational fluid dynamics (CFD) is applied to spraying processes with strong enthalpy coupling. Focus is brought to industrial scale applications in the field of environmental engineering. A transient 3D finite volume solver is used, wherein the disperse phase is modeled within an Lagrangian framework. Two-way mass and enthalpy coupling is taken into account. Resulting limitations of the traditional sequential model droplet integration approach are discussed, which potentially lead to thermodynamically inconsistant or oscillatory solutions, especially in zones of dense spray. As an alternative a combined sequential-simultaneous solution algorithm is proposed. Thus obtained results show sufficient aggreement with a validated test case. Application to industrial scale reactors in the field of flue gas cleaning are demonstrated exemplarily.

INTRODUCTION

The application of Computational Fluid Dynamics (CFD) as a means to support reactor design activities as well as subsequent optimization tasks is getting increasingly popular in the field of plant engineering.

Flue gas cleaning processes are an illustrative example out of the range of environmental technologies. Frequently water with or without other reactants is injected into the flue gas stream. The specific temperature levels depend on the technology applied. In case of the selective non catalytic reduction (SNCR) this occurs at temperatures from 800°C to 1000°C directly after the primary combustion chamber. The time span, that is needed to evaporate the NH_3/liquid-mixture, determines the penetration depth of the spray and consequently – among other parameters – the spatial distribution of the reactant. Similar effects have to be considered in the selective catalytic reduction process (SCR), where ammonia is injected into the exhaust gas at temperatures from 300°C to 400°C.

Semi-dry desulphurization plants with $Ca(OH)_2$ as quasi-dry reactant are typically operated at temperatures around 150°C and elevated vapor saturation levels. Water is applied to quench the entering gas stream and additionally to activate the surface of the solid sorption medium.

NOMENCLATURE

A	[m²]	Exchange area of droplet surface
c_p	[J/(kgK)]	Specific heat at constant pressure
j	[kg/(m²s)]	Specific mass flow
$\hat{H}_L$	[J/kg]	Heat of evaporation
H	[J]	Enthalpy
n_p	[-]	Number of parcels
N_d	[-]	Number of particles per computational parcel
m	[kg]	Mass
q	[J/(m²s)]	Specific heat flow
Q	[J/s]	Heat transfer rate
S_h	[J]	Enthalpy source
S_m	[kg]	Mass source
S_φ		Source term for scalar quanity φ
t	[s]	Time
Δt_e	[s]	Integration time step for continuous phase
T	[K]	Temperature
w	[kg/kg$_{total}$]	Vapor concentration
x	[m]	Particle diameter

Special characters

α	[W/(m²K)]	Heat transfer coefficient
α_c	[-]	Volume fraction of continuous phase
ρ	[kg/m³]	Density

Subscripts

c	Continuous phase
d	Droplet
i	Counter for ith droplet
s	Surface
v	Vapor
0	Bulk or reference

Exact adjustment of the water injection to the flue gas parameters is necessary to ensure high cleaning efficiency and to avoid undue corrosion. Wet desulphurization is accomplished by physical and chemical absorption of the SO_2 by the injected slurry droplets. Due to the high liquid mass flux, the spatial distribution of the spray can also be used to create a uniform gas flow.

This short summary shall give an idea of the manifold applications of CFD, as long as efficient models and solution strategies are provided. The modelling of sprays is best accomplished by Eulerian-Lagrangian solvers. The Lagrangian framework in principal allows to consider each particle separatly with its individual properties. For the correct handling of problems in conjunction with the above mentioned technologies, it is inevitable to consider heat and mass transfer effects, namely evaporation and condensation. In this work an alternative to the widespread sequential solution strategy is presented and its potentialities are demonstrated.

MODEL FORMULATION

As numeric platform the commercial CFD-package FIRE 7.3 is used. It features a transient 3D finite volume solver for Reynolds-averaged transport equations on unstructured grids. A prototype of such a transport equation for the generic scalar variable φ is given in equation (1).

$$\frac{\partial \alpha_c \rho_c \varphi}{\partial t} + \mathrm{div}(\alpha_c \rho_c \varphi \cdot \vec{\mathbf{v}}) = \mathrm{div}(\mathrm{grad}\ \varphi) + S_\varphi \qquad (1)$$

The problem specification requires the consideration of mass, momentum and enthalpy conservation equations. The corresponding continuous flow field solution is calculated by applying the SIMPLE algorithm [1] and a fully implicit transient integration scheme.

Particles and droplets are modelled in a Lagrangian framework, where a specified number N_d of dispersed particles of the same type and identical properties are grouped to parcels or computational droplets. This process, that is denoted as disperse phase discretization, thus permits numerical treatment of industrial scale problems with increased dispersed mass. Phase coupling is accomplished by the application of the particle source in cell method (PSIC) [2]. The individual contributions of each parcel in a specific control volume are calculated in the Lagrangian framework and then mapped back to the continuous transport equation via the corresponding source term S_ϕ.

The applicability of transient solution algorithms to industrial scale problems is greatly influenced by constraints in the choice of the global integration time step Δt_E, which are inherently connected to the solution methods and the underlying physical problem to be solved. Considering solely the continuous phase solver of FIRE (S_ϕ=0) the integration time step Δt_E is limited by a Courant-number criterion.

Model equations for a single computational droplet

Likewise to the continuous field equation a proper set up disperse phase model for the problem specification has to consider mass, enthalpy and momentum transfer. The latter is obtained from Newton's second law of motion, taking into account the gravity force f_g, the drag force f_d and the buoyancy force f_b. Thus the equations defining the parcel velocity (equation 2) and position (equation 3) are obtained.

$$\frac{d\mathbf{v}}{dt} = f_g + f_r + f_b \qquad (2)$$

$$\frac{d\mathbf{x}}{dt} = \mathbf{v} \qquad (3)$$

Heat and mass transfer is modelled following an approach of Dukowicz [3], which allows the evaluation of the parcel temperature and mass evolution as a function of the heat transfer rate Q_c and the ratio of the mass and enthalpy fluxes $j_{v,s}/q_s$ at the droplet surface.

$$Q_c = A \cdot \alpha \cdot (T_0 - T_{d,s}), \qquad (4)$$

$$\frac{dT_{d,s}}{dt} = \frac{Q_c}{m_d \cdot c_{p,d}} \cdot \left(1 + \hat{H}_L \cdot \frac{j_{vs}}{q_s}\right) \qquad (5)$$

$$\frac{dm_d}{dt} = Q_c \cdot \frac{j_{v,s}}{q_s} \qquad (6)$$

The underlying applied analogy of heat and mass transfer is valid under the assumption of (a) constant Lewis number and (b) uniform conditions at the droplet surface. Additionally, in this approach a spherical shape and an ideal mixing within the droplet is assumed. Thus the droplet surface temperature $T_{d,s}$ in the formulae (4) and (5) can be replaced by an unique droplet temperature T_d. The restriction to spherical droplets allows the calculation of the overall heat transfer coefficient using correlations based on Nusselt and Sherwood numbers. The transport processes are driven by the temperature gradient $(T_0 - T_{d,s})$ and the concentration gradient $(w_0 - w_{d,s})$ over the droplet's boundary layer. The latter is hidden in the term $j_{v,s}/q_s$, underlying the assumption of total saturation at the droplet surface [3].

Eventually the source terms for the phase coupling have to be specified. Since the focus is brought to heat and mass transfer the evaluation of the momentum source is not discussed here. The mass source is simply defined as the integral contribution of each droplet following equation 6 multiplied by the number of droplets $N_{d,I}$ belonging to the corresponding parcel.

$$S_m = -\sum_{i=1}^{n_p} N_{d,i} \cdot \Delta m_{d,i} \qquad (7)$$

The enthalpy source term can be evaluated in two different ways depending on the reference point of view. We consider the total gas enthalpy in the cell, which is defined as follows:

$$H_c = m_c \cdot c_{p,c} \cdot T_c \qquad (8)$$

Then the differential change of the enthalpy content within the control volume is derived by differentiating equation 8 and application of the chain rule. Under the assumption of constant specific heat and switching to finite differences, the enthalpy source term evaluates to

$$S_h = S_m \cdot c_{p,c} \cdot T_c + m_c \cdot c_{p,c} \cdot \Delta T_c \qquad (9)$$

The problem in this formulation is the fact that the information on the change of the temperature in the control volume is not always accessible. An alternative formulation makes use of the enthalpy balance between disperse and gaseous phase (equation 10), considering the control volume as adiabatic system:

$$S_h = \hat{H}_L \cdot S_m + S_m \cdot c_{p,c} \cdot T_0 - \sum_{i=1}^{n_p} N_{d,i} \cdot \Delta H_{d,i} \quad (10)$$

Here the first term on the right hand side defines the latent heat, the second the transferred enthalpy due to mass transfer. The last term specifies the net total enthalpy difference of the considered parcels. For a single parcel equation the number of parcels n_p is 1. With the equations 4 and 5 the enthalpy source term can be eventually formulated as follows:

$$S_h = S_m \cdot \left(\hat{H}_L + c_{p,c} \cdot T_0\right) - \sum_{i=1}^{n_p} N_{d,i} \cdot \left(Q_{c,i} \cdot \Delta t\right) \cdot \left(1 + \hat{H}_L \cdot \frac{F_{vs}}{q_s}\right)_i \quad (11)$$

Sequential versus simultaneous integration approach

The workflow of the standard sequential integration procedure is shown on the left side of Figure 1. In a first step the path line of a single parcel is computed, followed by an update of its position and velocity. After that the changes of the droplet energy and mass are obtained by integrating equations (5) and (6). This procedure is executed for any individual droplet. During the whole integration time step Δt_e the properties of the gas field are kept constant, thus forming a constant reference state (T_0, w_0) for the calculation of the driving forces in equations 5 and 6. Especially in regions with strong enthalpy and mass coupling (e.g. dense sprays, where its volume fraction exceeds 5%) the assumption of a constant reference state becomes easily violated due to excessive source terms. This commonly leads to thermodynamic inconsistent results, where even the direction of mass and enthalpy transfer can become reversed for some droplets. In the worst case, oscillations in the solution can force an abort of the simulation.

Evidently a stable and thermodynamic correct solution can only be maintained, if an update of the continuous phase properties is carried out more frequently. Hence, the global Eulerian integration time step Δt_e has to be reduced to meet this requirement, even if the potential numerical inconsistency is limited to a single control volume.

To overcome this problem an alternative solution algorithm was proposed by Aguayo and Weiß [4]. They suggest to switch to a combined sequential-simultaneous approach (cf. Figure 1), where in a first step the sequential integration for all parcels is carried out. In a second stage the algorithm changes to a cellwise simultaneous integration procedure, taking into account all parcels that are located in the concerning cell and additionally the gas phase itself. Thus a system of $(2 \cdot n_p + 2)$ ordinary differential equations (ODE) is set up for each control volume - $2 \cdot n_p$ ODEs for the droplet phase (equations 5 and 6 for each droplet) plus 2 equations which account for the gas phase:

$$\frac{dm_c}{dt} = -\sum_{i=1}^{n_p} N_{d,i} \cdot \frac{dm_{d,i}}{dt} \quad (12)$$

$$\frac{dH_c}{dt} = -\sum_{i=1}^{n_p} N_{d,i} \cdot \left(Q_{c,i} + \frac{dm_{d,i}}{dt} \cdot c_{p,c} \cdot T_c\right) \quad (13)$$

The system is solved by a Runge-Kutta-Fehlberg integration procedure with adaptive time stepping [5]. Gas phase modifications are carried out in form of temporary updates, which are only accessible within the Runge-Kutta routine itself. The regular update of the gas flow field variables still occurs in the continuous solver part (cf. Figure 1), whereas the corresponding source terms are available directly from net difference after the integration following the equations 12 and 13. The major improvement of the combined approach is the change from a global to a local time step criterion. Thus the frequency of the reference state update ($T_0(t_{RK})$, $w_0(t_{RK})$) becomes a function of the time stepping in the Runge-Kutta algorithm. Nevertheless, the new approach suffers from an implicit time discretization restriction as well. It is based on the underlying assumption, that the droplet positions and velocities remain constant throughout the simultaneous integration of the mass and enthalpy ODE system.

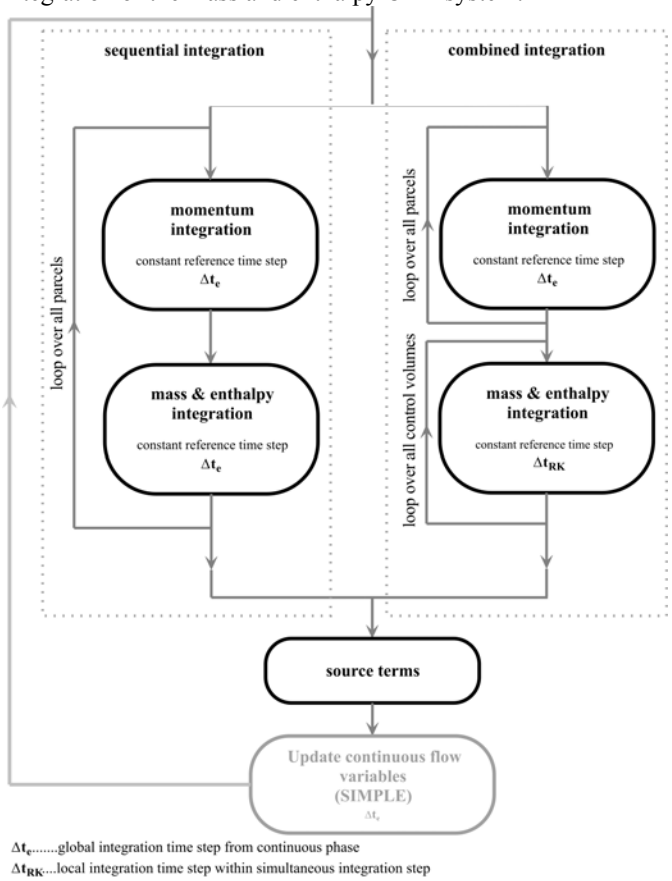

Figure 1 Schematic workflow of the sequential and combined integration approach

RESULTS

Droplet ensembles in a single control volume cell

In this section a single control volume with a relatively small fraction of disperse phase volume is examined. (cf. Figure 2a). Both integration approaches were validated against each other considering a very dilute configuration and showed very good agreement. Next, a denser spray configuration was chosen. Strong enthalpy and mass coupling was forced by the choice of the initial conditions of the system, which are shown in Figure 2 b.

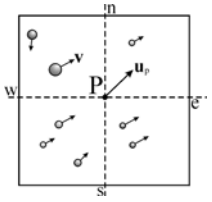

(a)

Droplets (n_p =4)					Gas (α_c = 0,96)	
ID	$N_{d,i}$	$\lvert v_{rel}\rvert$	$x_{d,ini}$	$T_{d,ini}$	V_c	1 m³
1	$6 \cdot 10^8$	20 m/s	500 µm	300 K	$T_{0,ini}$	334 K
2	$8 \cdot 10^8$	10 m/s	50 µm	290 K	p	1 bar
3	$20 \cdot 10^8$	0 m/s	120 µm	298 K	$w_{0,ini}$	8 kg/kg
4	$50 \cdot 10^8$	0 m/s	120 µm	360 K	φ	63 %

(b)

Figure 2 Sketch of a single control volume with its particulate cell inventory (a); Configuration of the single cell testcase (b)

Again transient simulations were carried out both with the sequential as well as with the combined integration procedure. The dependence of the quality and stability of the solution on the size of the global integration time step was tested by varying the global continuous integration time step Δt_e from 1 ms to 6 ms. The individual temperatures of the involved phases were plotted against the vapor mass fraction in the control volume (cf. Figure 3). In the same manner the equilibrium line was drawn, thus allowing the distinction of zones, where unexceptionally evaporation or condensation (coloured in blue) takes place. Additionally, the driving gradients can be assessed by the difference on the abscissa or ordinate from the considered droplet or gas state to the equilibrium line. The results are shown in Figure 3. For reasons of clarity only two droplets were considered, either of them in the evaporation regime (droplet 4 denoted by red lines in Figure 3). Considering the solution by the combined integration as the frame of reference, more or less severe deviations are obtained, which increase proportionally with the global integration time step.

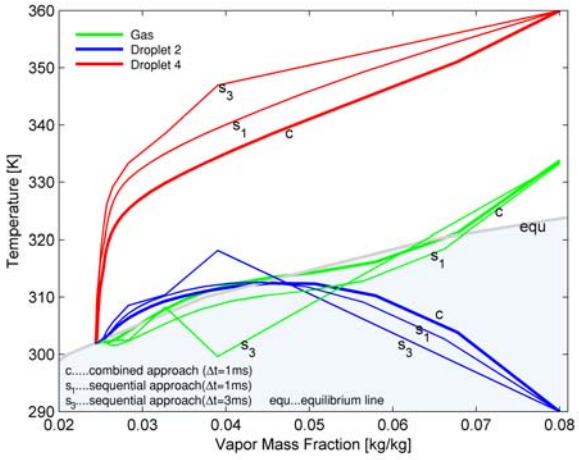

Figure 3 Driving gradients for the transfer processes

Especially the solution of the second droplet and the gas phase show an onset of instability when a global time step of 3 ms was used. An increase to 6 ms eventually lead to heavy osciallations of the solution and hence to an abort of the sequential solving procedure, which is illustrated in Figure 4. The combined solution, however, decreased in quality but still showed the same overall tendency.

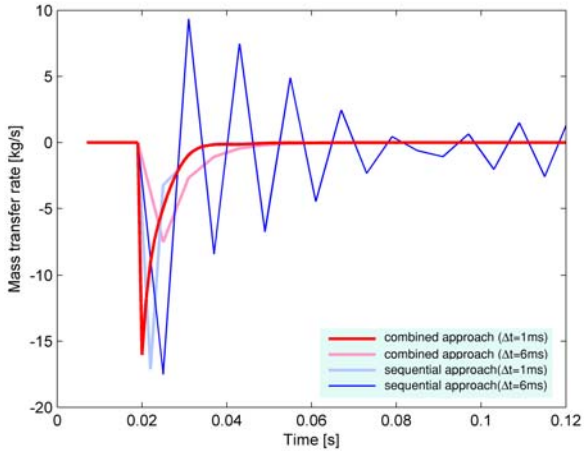

Figure 4 Instable, oscillating solution obtained by sequential integration of the droplet model

Validation case: Evaporating spray [7]

The combined integration approach was tested by simulating an lab-scale atomizer for the sytem isopropyl-alcohol and air [6]. The basic configuration is sketched in Figure 5 [7]. The turbulent properties of the continuous flow field were modelled by the standard k-ε model. Additionally an isotropic Eddy-Lifetime approach [8] was chosen to account for turbulent dispersion effects on the droplets. Turbulence modulations of the continuous field due to the presence of the droplets were not modelled. Enthalpy and mass coupling was considered by the model equations published in [4, 6], which slightly differ from that provided in the current work. The injection condition for the model droplet ensemble are generated, neglecting any possibly existent correlation (cf. [10]) between the droplet size and the droplet velocities.

The results were validated against experimental data [7, 9] and numerical simulation results [10].

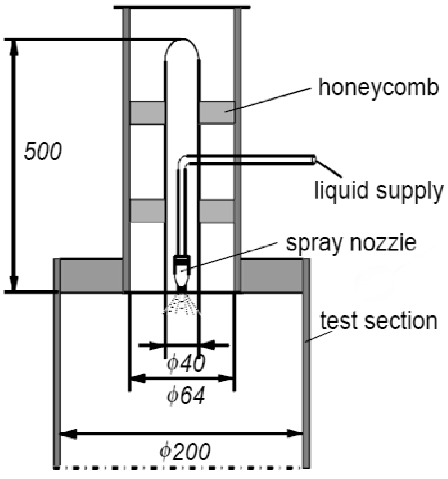

Figure 5 Atomization configuration [7]

Exemplarily the spatial distribution of the droplet diameter is shown in Figure 6. Especially in the region near the nozzle tip and further downstream near the centreline – both regions

where a higher disperse phase fraction can be presumed – a good agreement is observed. The increasing deviations in the radial coordinate are mainly attributed to effects originating from the insufficient description of the turbulent dispersion related quantities [6] in comparison to the reference case by Chen&Pereira [10].

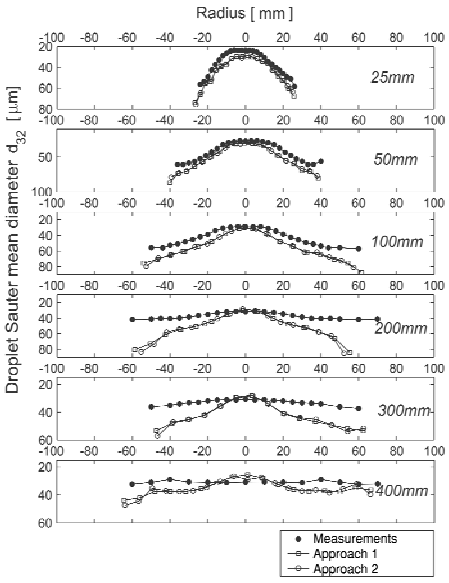

Figure 6 Spatial evolution of the droplet Sauter diameter

Simulation of an industrial scale spray condenser

In this section the findings from the single control volume test case shall be transferred to an industrial scale problem. Therefore a spray condenser is chosen to be numerically analyzed [4, 6]. The functionality of a condenser in general includes the quenching of a vapour laden gas stream by a cold water jet until the saturation level is reached. Simultaneously the absolute vapour fraction of the gas is reduced by condensation. Basic data of the present problem is given in Figure 7.

Operating data		
Gas flow rate	62000	m^3/h
Temperature of gas feed	95	°C
Static pressure at the gas entrance	1	bar
Absolute humidity of gas feed	0.12	kg/kg_{total}
Total injected liquid volume flux	161	m^3/h
Liquid injection temperature	25	°C
Droplet start velocity	7 – 9	m/s
Number of liquid injection nozzles	8	-
Sprays Sauter diameter	d_{32}=980	µm
	d_{10}=300	µm
Calculation domain		
Height	8	m
Diameter	2,5	m
Number of cells	221758	-
Minimum cell volume	50	cm^3
Maximum cell volume	300	cm^3

Figure 7 Operating data of condenser

At first simulations were carried out with the sequential approach. The global integration time step Δt_e was chosen to be very short (0,5ms) to avoid numerical problems due to oscillating solutions as discussed above. Assuming a total simulation time of at least 10 seconds this would have required a total number of 20.000 time steps. Nevertheless a stable solution could not be obtained. As shown in Figure 8, local temperature levels below the water triple point were observed. These errors are augmented by problems coming from the update of all temperature dependent phase properties.

As it turned out numerical problems occurred mainly in the upper part of the condenser in the vicinity of the spray banks, where dense spray regions are likely.

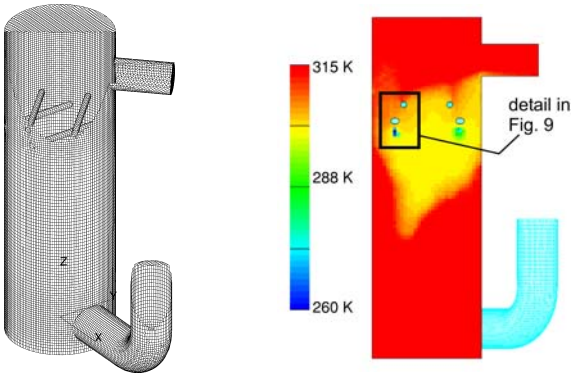

Figure 8 Condenser geometry with spray banks and temperature profile at 1,45 s after start of spray injection

Consequently investigations were focused on the flow characteristics in that zone. Figure 9 shows the droplet motion and the corresponding temperature profile in the vicinity of two spray banks. Obviously one nozzle is arranged in a manner, such that the spray is – at least partly - injected onto the subjacent spray bank, which leads to extremely high liquid mass in the neighbouring cells of the surface (Figure 9, left).

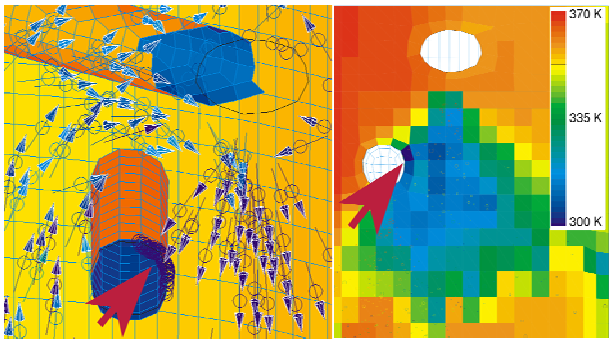

Figure 9 Droplet motion and temperature profile (center values of control volumes) around the spray banks (details according to Figure 8). The spatial discretization is indicated by the checkerboard pattern in the temperature profile. Arrows indicate the relevant cell zone

Combined with the fine spatial discretization, that is necessary to resolve the geometrical details adequately (depicted by the graphical resolution in Figure 9, right), the

relative impact of the local source terms on the gas field is increased. Hence, the lowest and possibly unphyiscal temperature values are obtained in the environment around the spray banks. This is a perfect example for a configuration, where a small local phenomenon influences the stability and eventually the feasibility of the simulation as a whole. A further reduction of the global time step would probably have resulted in excessive computational costs.

As a consequence, the combined integration approach was applied. Due to the assumption of a constant droplet inventory of each cell during the simultaneous integration process, this restriction has to be checked in advance of any calculation to assure, that the significant phenomena are temporally resolved. In this case the minimum edge length within the geometry was assessed from the smallest volume assuming cubic cells. Thus an approximate length of 3,5 cm is derived. Considering the initial droplet velocity provided by Figure 7 a maximum time step in the order of magnitude of 5 ms is evaluated. This value was then used as global time step in the simulation, which was carried out without any problems. The temporal evolution of the temperature field is shown exemplarily in Figure 10.

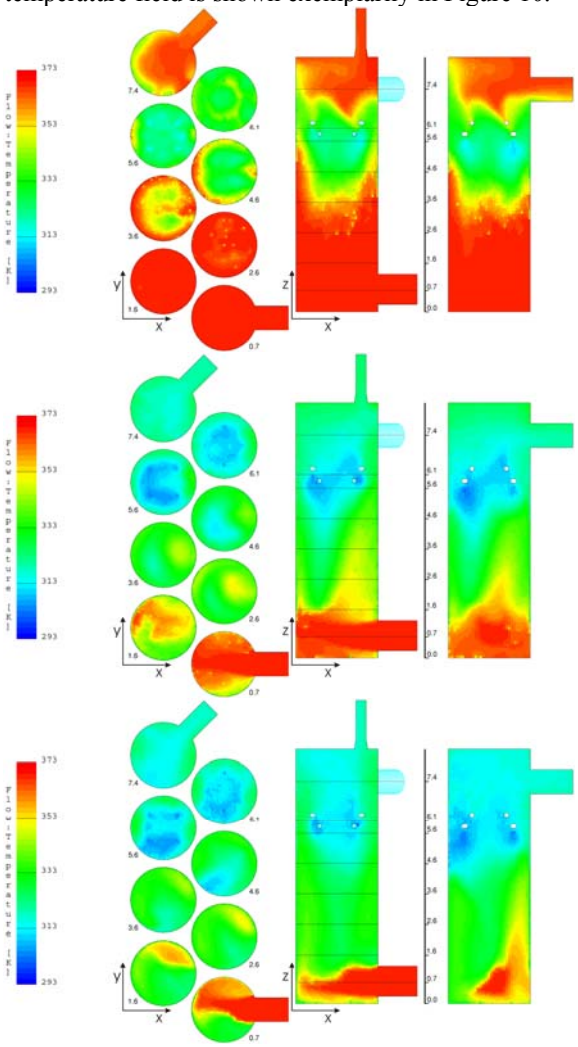

Figure 10 Temporal evolution of temperature field 0,7 s, 2,1 s and 5,6 s after start of spray injection

CONCLUSION

An alternative solution strategy within the Eulerian-Lagrangian framework for strongly enthalpy and mass coupled polydispers droplet laden gaseous flows was presented. On a single control volume configuration the gain of numerical stability compared to the widespread sequential approach was shown. As main drawback of the latter method the prerequisite of a small impact of the enthalpy and mass source terms to the continuous phase was identified, which as a consequence results in a possibly tremendous restriction to the global integration time step and at the same time to excessive computational costs.

The switch to the presented combined sequential-simultaneous algorithm allows to consider this restriction on the local level of the individual control volume. On the other hand a new global time step criterion is introduced, resulting from the assumption of a constant droplet inventory of the control volume. In contrast to the sequential approach, a violation of the criterion does not effect the stability but the quality of the solution.

REFERENCES

[1] Patankar, Numerical heat transfer and fluid flow. (1980). Hemisphere Publishing Cooperation.

[2] Crowe, Sommerfeld and Tsuji, Multiphase flows with droplets and particles. (1998). CRC Press.

[3] Dukowicz, Quasi-steady droplet phase change in the presence of convection. (1980). Los Alamos Scientific Laboratory.

[4] Aguayo and Weiß, Enthalpy two way coupling for near vapor saturated polydispersed spray flows. Proceedings of the 5th International Conference on Multiphase flows (ICMF)], paper 393. Yokohama. (2004)

[5] Press et al., Numerical recipes in C - The art of scientific computing. 2nd edition. (2002). Cambridge university press.

[6] Aguayo, Droplet phase change phenomena in CFD simulations of wet scrubbers and quenching processes, (2005)

[7] Sommerfeld et al., Spray evaporation in turbulent flow. [Proceedings of the 2nd Symposium on Engineering, Turbulence Modeling and Measurement], pp. 935-945. (1993).

[8] Gosmann and Ioannides, Aspects of computer simulations of liquid fuelled combustors. AIAA, 81-0323. (1981).

[9] Sommerfeld and Qiu, Experimental studies of spray evaporation in turbulent flow. Int.J.Heat and Fluid Flow, 19, pp. 10-22. (1998)

[10] Chen and Pereira, Computation of turbulent evaporating sprays with well-specified measurements: a sensitivity study on droplet properties. International Journal of Heat and Mass Transfer, 39, pp. 441-454. (1996).